The FASEB Journal

FASEB
Federation of American Societies for Experimental Biology

RESEARCH ARTICLE OPEN ACCESS

CXCL14 Chemokine Exacerbates Acute Viral Hepatitis in Coronavirus MHV-Infected Mice and Is Associated With Human Acute Viral Hepatitis

Christelle Devisme[1,2,3] | Claire Piquet-Pellorce[1] | Arnaud Chalin[1] | Benjamin Lefevre[1] | Charlotte Pronier[4] | Vincent Thibault[4] | Jacques Le Seyec[1] | Céline Raguénès-Nicol[1] | Charaf Benarafa[2,3,5] | Michel Samson[1]

[1]University of Rennes, Inserm, EHESP, Irset (Institut de recherche en santé, environnement et travail)—UMR_S 1085, Rennes, France | [2]Institute of Virology and Immunology, Mittelhäusern, Switzerland | [3]Department of Infectious Diseases and Pathobiology, Vetsuisse Faculty, University of Bern, Bern, Switzerland | [4]University of Rennes, CHU Rennes, Inserm, EHESP, Irset (Institut de recherche en santé, environnement et travail)—UMR_S 1085, Rennes, France | [5]Multidisciplinary Center for Infectious Diseases, University of Bern, Bern, Switzerland

Correspondence: Michel Samson (michel.samson@inserm.fr)

Received: 25 July 2024 | **Revised:** 4 April 2025 | **Accepted:** 22 April 2025

Funding: This work was supported by the INSERM, the "Ministère de l'Enseignement Supérieur, de la Recherche et de l'Innovation", the University of Rennes, and the "Région Bretagne" and in particular the CPER grant called "infectio". C.D. was supported by a PhD fellowship from the "Région Bretagne", INSERM, and ANRS.

Keywords: acute viral hepatitis | alarmin | chemokine | CXCL14 | human blood sample | immune response | mouse animal

ABSTRACT

Deaths from viral hepatitis continue to rise around the world due to the lack of early biomarkers. We aimed here to evaluate the chemokine CXCL14, as a novel biomarker in acute viral hepatitis. We used a mouse model of acute hepatitis induced by murine hepatitis virus (MHV), a hepatotropic and lytic coronavirus, and showed that CXCL14 is overexpressed in the liver and sera of infected mice. Using primary cultures of murine and human hepatocytes, we showed that hepatocytes are the main source of CXCL14 after lytic hepatotropic virus infection and that CXCL14 expression is also induced by the pro-inflammatory cytokines IL-6 and TNFα. CXCL14 KO mice infected with MHV were partially protected and showed an attenuated antiviral immune response compared to wild-type mice. Finally, we show that CXCL14 is overexpressed in the sera of human patients infected with hepatitis viruses A, B, and E or herpes simplex virus. A positive correlation between CXCL14 and ALT levels in the sera of patients with acute herpetic hepatitis, as well as in mice models, suggests that hepatocyte lysis is necessary for the release of CXCL14. Overall, these data highlight that CXCL14 expression is associated with the occurrence of acute viral hepatitis and could be considered an alarmin and a new indicator of inflammation. CXCL14 serum levels are also associated with the severity of viral-induced liver injury.

1 | Introduction

The number of people dying from infection with hepatitis viruses continues to increase worldwide, representing a major global public health and economic problem [1]. Hepatitis B virus (HBV) and hepatitis C virus (HCV) are the main causes of viral liver infection, with 354 million people affected, as estimated by the World Health Organization in 2024 [2]. HCV and HBV

Abbreviations: ALT, alanine aminotransferase transaminase; AST, aspartate aminotransferase transaminase; AUC, area under the ROC Curve; Dpi, day post-infection; HAV, HBV, HCV, HDV, and HEV, hepatitis A, B, C, D, or E virus; Hpi, hour post-infection; HSV, herpes simplex virus; IFN, interferon; IL, interleukin; KO, knock-out CXCL14$^{-/-}$; MHV, mouse hepatitis virus; MOI, multiplicity of infection; NI, non-infected; NK, natural killer; OSM, Oncostatin M; TNF, tumor necrosis factor; WT, wild-type CXCL14$^{+/+}$.

may trigger chronic hepatitis, characterized by persistence of the virus and fibrosis, with a risk of hepatocellular carcinoma development. However, HAV, HBV, HDV, HEV, herpes simplex viruses (HSV-1 or HSV-2), and, to a lesser extent, HCV are also responsible for acute liver failure or fulminant hepatitis, leading sometimes to a potentially lethal liver dysfunction. In this situation, patients rapidly develop liver failure, associated with encephalopathy, that will eventually lead to death in the absence of liver transplantation [3].

Viral hepatitis is characterized by inflammation and the mobilization and activation of molecular and cellular actors of the immune system. Thus, cytokines play a key role in controlling the infection. In the liver, resident immune macrophages, called Kupffer cells, are responsible for the release of cytokines, such as TNFα, IL-1β, and IL-6 [4, 5]. In acute hepatitis, innate immune cells from the liver, in particular NK and NKT cells, constitute the major immune cell population of lymphocytes and play a particularly important role in the pathogenesis of viral hepatitis [6]. Various types of IFNs, such as IFN-α, IFN-β, or IFN-γ, are cytokines produced by immune cells and hepatocytes and are involved in the inhibition of the replication of hepatitis virus in the liver [7, 8]. In addition, chemokines, a large family of cytokines, are involved in hepatitis by recruiting immune cells from the blood to the liver and then activating them in the liver [4, 9].

CXCL14, also called BRAK (breast and kidney expressed chemokine), is a relatively recent member in the family of homeostatic chemokines [5]. The amino-acid composition of CXCL14 is well conserved between many species [10]. Murine CXCL14 has 97.4% sequence homology with human CXCL14, differing by only two amino-acid residues [11]. A recent study reported that CXCL14 can bind and activate the orphan MAS-related G protein-coupled receptor X2 (MRGPRX2) principally expressed on mast cells [12]. The CXCL14 receptor on other cell types remains elusive, and thus, its intracellular signaling pathway and functions are not fully understood for any species. CXCL14 is constitutively expressed in several tissues and organs, such as breast, kidney, lung, skin, and liver [13]. Such basal expression suggests that CXCL14 plays a role in homeostasis and immune surveillance [10, 14]. Furthermore, it has been shown to be a chemoattractant for blood monocytes [15], macrophages, immature dendritic cells [16], and NK cells [17]. Minimally, CXCL14 expression appears to correlate with inflammatory processes, and this chemokine has been shown to have direct antimicrobial activity [15, 18].

An experimental model of acute hepatitis has been developed in mice by infection with mouse hepatitis virus (MHV) [19, 20], which also has the ability to invade the brain like other coronaviruses [21]. MHV type 3 (MHV-3) produces a clinically relevant model of acute hepatitis in infected mice, resulting in fulminant hepatitis, liver failure associated with substantial hepatocyte necrosis, and death 5–7 days after infection [22, 23]. MHV type A59 (MHV-A59) induces a mild form of acute hepatitis in mice in 3 days, with an effective immune response. However, MHV-A59 is not inducing death of the animals and leads to a recovery in 10 days. MHV infections can therefore serve as models to decipher the viral and immunological events of acute hepatitis [24, 25]. In this context, a preliminary experiment highlighted an overexpression of CXCL14 mRNA following MHV-3 inoculation in C57Bl/6J mice.

Here, we aimed to study the expression and function of the CXCL14 chemokine during viral hepatitis using various approaches combining in vitro assays of primary hepatocyte cultures infected by lytic viruses and in vivo assessment of CXCL14 in murine models of viral hepatitis and human acute hepatitis.

2 | Materials and Methods

2.1 | Human Samples

The study protocol was approved by the ethics committee of Pontchaillou University Hospital (Rennes, France), and written informed consent was obtained from all participants. Inclusion criteria were any acute liver injury with alanine aminotransaminase (ALT) activity > 129 IU/L (equivalent to three times the upper normal limit, considered in this study to be 43 IU/L). Patients with acute-on-chronic liver injury were excluded or if another source of ALT activity was suspected (rhabdomyolysis, myocardial infarction, etc.). None of the patients had hepatocellular carcinoma. A control group consisting of 36 healthy volunteers from the French Blood Institute (Rennes, France), who were not infected by HBV, HCV, and Human Immunodeficiency Virus, and had normal ALT activity (< 43 IU/L), was also included. Human serum was obtained at the time of entry into the study and stored at −80°C until further analysis.

2.2 | Ethics Declarations of Animal Experiments

All experimental protocols on animals were conducted in compliance with French and Swiss Animal Welfare legislation and the institution's guidelines for animal welfare. Authors were authorized to conduct animal experimentation by “La direction des Services Vétérinaires” (license M. Samson, #A3523840) and by the Commission for Animal Experimentation of the Cantonal Veterinary Office of Bern (license C. Benarafa BE22/18). The project was authorized by the “Comité Régional d'Ethique d'Expérimentation Animal” [CREAA] and the license given by the “Ministère de l'Education Nationale et de la Recherche” (#21301-2019062102252380). The animals were kept in individually ventilated cages in environmentally controlled rooms and had access to water and food ad libitum.

2.3 | Generation of CXCL14$^{-/-}$ Mice

CXCL14-deficient knock-out (KO CXCL14$^{-/-}$) mice previously described [13] were further backcrossed to at least five generations in a C57BL/6J background. The current colony was generated by rederivation of frozen embryos, and all experimental mice were obtained from breeding heterozygous (CXCL14$^{+/-}$) mice in the animal facilities (Institute of Virology and Immunology, Switzerland). Genotyping was performed by diagnostic PCR using genomic DNA from ear punches and specific primers for wild-type (WT;

forward: 5′-TGGCCCAGGAATCAAACACAG-3′; reverse 5′-GGGGCCCTCCTACTTCTACCATC-3′) and CXCL14$^{-/-}$ alleles (forward: 5′-CTTGGGTGGAGAGGCTATTC-3′; reverse 5′-CAAGGTGAGATGACAGGAGATC-3′). Genotypes of pups born from heterozygous matings were determined at weaning (3-week-old). Importantly, KO mice did not present any noticeable phenotype compared with WT littermates from weaning age to the time of infection.

2.4 | Mouse Infection Studies

Amplification of MHV-3 and MHV-A59 was obtained on L2 cells as described [21]. MHV-3 infection was studied in C57Bl/6J mice, aged between 8 and 12 weeks. After a preliminary dose–response for each lot of MHV-3, a dilution was chosen that does not cause death before the fifth day of infection (called suboptimal dose). MHV-3 was diluted in sterile Dulbecco's phosphate buffered saline, and 200 μL/20 μg of mouse body weight was injected intraperitoneally. MHV-A59 infection was studied in mice, aged between 9 and 13 weeks, by inoculation with 5000 PFU of MHV-A59. Virus was diluted in sterile DMEM medium, and 200 μL/20 μg of mouse body weight were injected intraperitoneally. Control mice were injected with sterile buffer only (referred as NI control mice).

Mice were monitored every 12 h for body weight loss and clinical signs, for up to 7 days. At 3, 5, or 7 days post-infection (dpi), mice were euthanized, blood samples were collected by the retro-orbital route after ocular anesthesia, and sera were stored at −80°C until further analysis. Organs were aseptically dissected, fixed in 4% paraformaldehyde, and embedded in paraffin.

2.5 | Culture of Primary Murine and Human Hepatocytes

Primary mouse hepatocytes (PMH) were recovered from C57Bl/6J WT mice. Mice were anesthetized with a mix of xylazine and ketamine (10 and 60 mg/kg, respectively), and the liver was first washed and then perfused by the inferior cava vein route with a solution of collagenase, as previously described [26]. Hepatocytes were seeded onto collagen I-coated culture plates at a density of 10^5 cells/cm^2 [26]. Twenty-four hours after seeding, cells were infected by MHV-3 at a multiplicity of infection (MOI) of 1 (virus: cell ratio of 1:1) or were stimulated with the pro-inflammatory cytokines, IL-6 or TNFα at 5 ng/mL each. Supernatants and cell lysates were then collected every 12 h to perform analysis by RT-qPCR, western blotting, or ELISA.

Primary human hepatocytes (PHH) were recovered from patients of the Pontchaillou University Hospital (Rennes, France) by hepatectomy following liver metastasis with colorectal cancer. Human hepatocytes were seeded onto collagen-I-coated plates at a density of 2×10^5 cells/cm^2 in seeding medium: William's E medium (Gibco, Life Technologies) with 10% FBS (HyClone FetalClone III), 1% penicillin–streptomycin, 0.5% gentamycin, 1% L-glutamine, and 0.1% insulin (Sigma 15500). Twelve hours later, medium was replaced and enriched with 2% dimethyl sulfoxide (DMSO, Sigma) and 0.02% hydrocortisone hemi-succinate at 0.1 μg/mL (UPJOHN) [27]. Three days after seeding, cells were infected with HSV-1 at a MOI of 1 or stimulated with pro-inflammatory cytokines (IL-6, TNFα, IFNγ, Oncostatin M (OSM), and IL-1β) at 5 ng/mL each. Supernatants and cell lysates were taken every 12 h to perform analysis by RT-qPCR, western blotting, or ELISA.

2.6 | RT-qPCR From Cells in Culture or Liver Tissue

The protocol and conditions for RNA extraction, RT-PCR, and qPCR were similar as reported earlier [26] using specific primers for CXCL14, IL-6, and TNF [26]. Sequences of primers were the following: human *CXCL14* (F 5′-TCCCAACCTGAGGATTTCTG-3′/R 5′-TTGGGAACCTCACATGCTTC-3′); human *18S* (F 5′-CGCCGCTAGAGGTGAAATTC-3′/5′-TTGGCAAATGCTTTCGCTC-3′); mouse *Cxcl14* (F 5′-CTCGTTCCAGGCATTGTACC-3′/R 5′-GTGTAAGTGTTCCCGGAAGG-3′); mouse *Il6* (F 5′-CGATGATGCACTTGCAGA-3′/R 5’-CTCTGAAGGACTCTGGCTTTG-3′); mouse *Tnfa* (F 5′-AGATAGCAAATCGGCTGACG-3′/R 5′-CGAGTGACAAGCCTGTAGCC-3′); mouse *18S* (F 5′-TTGGCAAATGCTTTCGCTC-3′/R 5′-CGCCGCTAGAGGTGAAATTC-3′).

For the absolute quantification of the MHV3 genome by qPCR, a plasmid (pBAC-JHMV^{IA}), containing the entire genome of the neurotropic JHM strain of MHV, was used for calibration [26]. Primers for quantification were *N-mhv3* forward 5′-TGGAAGGTCTGCACCTGCTA-3′ and reverse 5′-TGGAAGGTCTGCACCTGCTA-3′.

2.7 | Western Blot

Protein extracts were obtained by disruption of cells in 25 mM Tris, 150 mM NaCl, 0.1% SDS, 0.5% sodium deoxycholate with protease inhibitors (cOmplete ULTRA Tablets, EDTA-free, Roche), and phosphatase inhibitors (PhosSTOP, Roche) and centrifugation for 15 min at 12 500 *g*. 30 μg of total protein extract was separated by 12% acrylamide SDS-PAGE and blotted on nitrocellulose. The membrane was incubated with a primary antibody against CXCL14 (1:2000, #ab137541 Abcam) and a secondary antibody goat anti-rabbit HRP (1:2000 Dako) or, using β-actin as a housekeeping protein, with a primary antibody against β-actin (1:5000, #A3854 Sigma) and a secondary antibody goat anti-mouse HRP (1:5000, Dako). Signal was revealed by ECL (Pierce).

2.8 | Transaminases, Chemokines, and Cytokines Detection in Fluids

ALT transaminase levels were measured according to the International Federation of Clinical Chemistry and Laboratory Medicine primary reference procedures at the Pontchaillou University Hospital (Rennes, France) or by following the

manufacturer's recommendations of the alanine transaminase activity assay kit (ab105134, Abcam).

CXCL14 was detected in sera and supernatants using a CXCL14 ELISA kit (DY866, R&D Systems) according to the manufacturer's instructions. A mouse CXCL14 standard curve was done with a mouse CXCL14 recombinant protein (#730-XC, Novus). The lower detection limit was 62.5 pg/mL for CXCL14. All samples were measured in triplicate.

Pro-inflammatory cytokines and chemokines were detected using the LEGENDplex Mouse Inflammation Panel (13-plex) array (Biolegend) according to the manufacturer's protocol. The lower detection limits are indicated on graphs. All samples were measured in duplicate.

2.9 | Immune Cell Analysis by Flow Cytometry

Liver immune cells were purified as previously described [23] and stained with LIVE/DEAD fixable green stain (#L34959 Life Technologies) and the following fluorochrome-conjugated antibodies: GR1-efluor 450 (1:100, #48-5931-82 eBioscience); CD4-BV510 (1:100, #561099 BD Pharmigen); TCR-BV605 (1:50, #562840 BD Pharmigen); CD19-BV786 (1:100, #563333 BD Pharmigen); CD69-PerCPCy5.5 (1:25, #104522 Biolegend); NK1.1-PEefluor (1:100, #61-5941-80 eBioscience); CD11b-PECy7 (1:200, #552850 BD Pharmigen); CD3-APC (1:50, #17-0031-81 eBioscience); and CD8-APC Cy7 (1:100, #557654 BD Pharmigen). Data were acquired using an LSRFortessa x20 flow cytometer (BD Biosciences) and analyzed using Flowlogic software (Inivai) with the gating strategy indicated in Figure S1.

2.10 | Histological Analysis

Formol-fixed paraffin-embedded tissue was cut at 4 μm and stained with hematoxylin–eosin (H&E) to investigate liver injury. Immunohistochemistry was performed with primary antibody raised against CXCL14 (1:200, #ab137541 Abcam), cleaved caspase 3 (1:200, #9661 Cell Signaling), myeloperoxidase (MPO, 1:1000 #A039829 Dako), FoxP3 (1:500, #bs-10211r Bioss), F4/80 (1:40, #12-4801-80 eBioscience), and secondary antibody accordingly as previously described [26]. Slides were scanned using a digital slide scanner (Hamamatsu Nanozoomer 2.0-RS) and the files analyzed using NDP viewer software (Hamamatsu).

2.11 | Statistical Analysis

Data are expressed as the means ± SD for all similar conditions. The mean values of individual data were analyzed using the non-parametric Mann–Whitney *U*-test. All in vitro experiments were analyzed using the parametric Student-*t* test. Receiver-operating characteristic (ROC) curve analysis was used as a global and standardized measure of the accuracy of predicting advanced hepatic fibrosis or cirrhosis. The ROC curve represents the plotting of sensitivity against specificity. All statistical analyses were performed using GraphPad Prism5 software.

3 | Results

3.1 | MHV-3 Infection Induces Hepatic and Serum CXCL14 Overexpression in Mice

We analyzed cytokine expression profiles following MHV-3 infection by performing quantitative PCR on a large series of 345 genes involved in inflammation during viral hepatitis using the previously described mouse fulminant-hepatitis by MHV-3 inoculation model [22]. The mice became ill as early as 2 days post-inoculation, with significant body weight loss, an increase in serum alanine (ALT) and aspartate aminotransferase (AST) transaminase levels, and major hepatocyte necrosis at 72 hpi, as expected (Figure S2). As shown in the first screen performed on 345 genes by our team [28], CXCL14 is clearly upregulated, as are a few other cytokines and chemokines. We then assessed CXCL14 mRNA expression by quantitative PCR in the livers of mice, infected or not with MHV-3, at various times post-inoculation. CXCL14 mRNA levels were five-fold higher in the livers of mice inoculated with MHV-3 at 48 and 72 hpi than in the non-infected (NI) controls (Figure 1A). Western blot analysis also showed that CXCL14 protein is constitutively expressed at a basal level in steady-state conditions, and their levels are increased in the livers of MHV-3-infected mice 48 and 72 hpi (Figure 1B). A major band was detected at 17 kDa, corresponding to the monomer of CXCL14 [27]. After quantification, CXCL14 production was significantly higher in the livers of MHV-3-infected mice 48 and 72 hpi than in those of NI mice (Figure 1C).

3.2 | Primary Murine and Human Hepatocytes Produce CXCL14

We next determined among hepatic cells whether hepatocytes could be the source of CXCL14 production. Cultures of primary murine hepatocytes were seeded and infected with various ratios of MHV-3 (MOIs of 0.5, 1, or 2). Non-infected hepatocytes had a polygonal appearance, with one or two nuclei (Figure 2A). Infection with MHV-3 at a MOI of 1 induced marked lysis of PMH after 5 days. We analyzed CXCL14 transcript levels in NI and infected PMH by quantitative PCR. No higher induction of CXCL14 mRNA expression was observed during the infection from day 2 to day 9 relative to NI hepatocytes. Next, we performed ELISA to quantify CXCL14 chemokine levels in conditioned media of NI and infected PMH over the time post-inoculation (Figure 2B), from 2 to 9 days post-infection. The level of CXCL14 was 500 pg/mL in conditioned media of NI cells (dotted line) and reached 2000 pg/mL at six days after MHV-3 infection with a MOI of 1. In parallel, the level of ALT in the same conditioned media showed a profile similar to that of CXCL14, with a peak at six days post-infection, suggesting a correlation between the release of CXCL14 and ALT (Figure 2C,D). We examined the potential regulatory pathway of CXCL14 expression by incubating PMH with IL-6 or TNF-α at 5 ng/mL and measuring CXCL14 mRNA levels by quantitative PCR. IL-6 induced a significant 12-fold increase in CXCL14 expression after 12–72 h of incubation (Figure 2E). Furthermore, TNFα induced a significant four-fold increase in CXCL14 transcript levels, with the maximum level obtained after 12 h of incubation (Figure 2F). CXCL14 was not found secreted in conditioned media of PMH incubating with IL-6 or TNFα only.

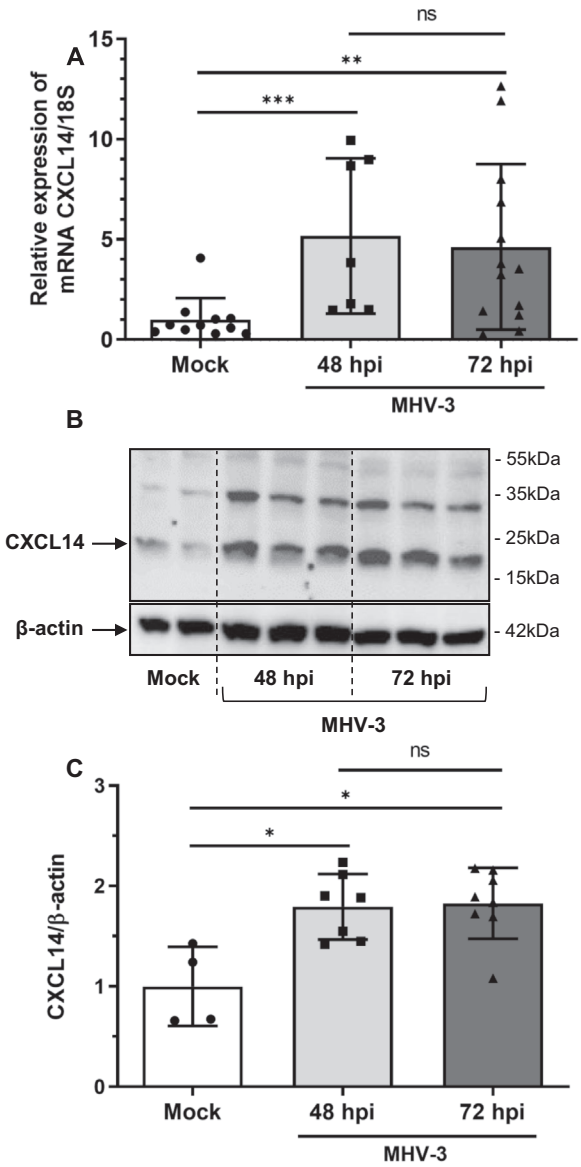

FIGURE 1 | Overexpression of CXCL14 in the livers of mice infected with MHV-3 at the mRNA and protein levels. Mice were injected intraperitoneally either with DPBS (Mock) or with MHV-3. 48 or 72 h after, mice were euthanized to harvest the liver. (A) CXCL14 mRNA expression in the livers of non-infected (Mock) and MHV-3-infected mice after 48 and 72 h. (B) Western blot analysis of CXCL14 in the livers of control (Mock) and MHV-3 infected mice 48 and 72 hpi. (C) Quantification of western blot of CXCL14 in the livers of control (Mock, $n = 4$) and MHV-3-infected mice 48 ($n = 7$) and 72 hpi ($n = 8$). A p-value < 0.05 was considered significant: *< 0.05, **< 0.01, ***< 0.001, ns not significant (comparison between mock mice and MHV-3 mice).

We further analyzed CXCL14 production in a human model by infecting PHH with HSV-1, at a MOI of 1 (Figure 3A). Non-infected PHH had a polygonal appearance, with mainly one nucleus and multiple contacts with other cells (Figure 3A, left). Seventy-two hours after HSV-1 infection, PHH became balloon-like, and multiple areas of lysis were observed (Figure 3A, right). Infection with HSV-1 induced a significant 12-fold increase in CXCL14 mRNA levels from 12 to 48 hpi in PHH (Figure 3B). CXCL14 release in the conditioned media of NI and infected cells from 12 to 72 hpi was measured by ELISA. CXCL14 was easily detectable at 12 hpi (300 pg/mL) and 72 hpi (100 pg/mL), whereas it was undetectable in the conditioned media of NI hepatocytes (Figure 3C). Furthermore, PHH were incubated, or not (NT), with a cocktail of five cytokines: IL-6, TNF-α, IFN-γ, IL1-β, and OSM, all at 5 ng/mL for 12–72 h. Cells were incubated with the five cytokines together because all are produced in response to viral infection, and furthermore, the amount of PHH was very limiting. The results showed that the cocktail of pro-inflammatory cytokines significantly induces CXCL14 mRNA expression within a few hours, with a maximum five-fold increase at 12 hpi (Figure 3D). We also studied the production of CXCL14 at the protein level by PHH and other human liver cells, such as primary hepatic stellate cells (HSC) [28] and a liver sinusoidal endothelial cells cell line (TRP3, RRID:CVCL_W908) [29] by western blotting. We were able to detect a band at 17 kDa corresponding to CXCL14 in PHH in non-treated conditions but not HSC or TRP3 (Figure 3E).

Overall, these in vitro experiments show that hepatocytes are a physiological source of CXCL14 in the liver and CXCL14 is expressed constitutively at a basal level that its expression is induced by TNF-α and IL-6 or other inflammatory cytokines and that its release by hepatocytes requires their lysis, as induced by infection with a lytic virus.

3.3 | CXCL14 Release Is Associated With Hepatocyte Death in MHV-3 Infected Mice

We inoculated MHV-3 in C57Bl/6J wild-type mice and then evaluated liver damage by H&E staining and cleaved-caspase 3 labeling of liver sections at 72 hpi (Figure 4A). The livers of NI mice showed no areas of lysis, whereas there were many areas of apoptosis in the livers of MHV-3-infected mice. We also evaluated liver damage by measuring ALT levels in the sera of NI and MHV-3-infected mice (Figure 4B). ALT levels fluctuated around 100 IU/L in NI mice, whereas they markedly increased up to 10 000 IU/L 3 days after MHV-3 inoculation. However, certain mice inoculated with MHV-3 had similar ALT levels to NI mice potentially due to the use of a suboptimal pathological dose of virus or due to a more efficient early immune response (gray colored dots) [23]. Nevertheless, all data points were analyzed as a single combined group. We also measured CXCL14 levels by ELISA in the sera of NI and MHV-3-infected mice (Figure 4C). The release of CXCL14 reached 100 pg/mL in the sera of NI mice and was significantly higher at 10 000 pg/mL in the sera of MHV-3-infected mice at 72 hpi. The serum levels of CXCL14 and ALT activity showed a significant exponential correlation, with $r^2 = 0.9065$, at 72 hpi with MHV-3 (Figure 4D). We also determined the serum concentrations of pro-inflammatory cytokines by multiplex immunoassay. IL-6 and TNFα levels were much higher in the sera of mice infected with MHV-3 at 72 hpi than those of NI mice, with mean levels of 1000 and 60 pg/mL, respectively (Figure S1). We also measured serum concentrations of IFNγ and IFNβ, cytokines mainly involved in the anti-viral response (Figure S3C,D). The levels of these cytokines were also higher in MHV-3-infected than NI mice with mean levels of 300 and 400 pg/mL, respectively. Finally, there was a

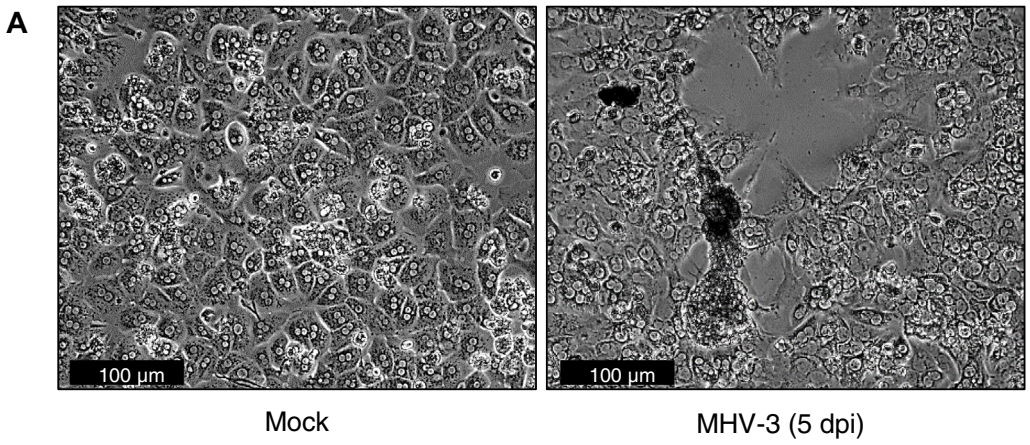

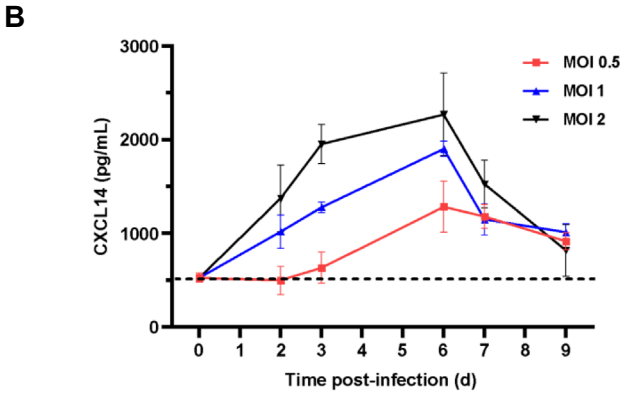

	D2	D3	D6	D7	D9
MOI 0,5	ns	ns	**	**	**
MOI 1	**	**	***	**	**
MOI 2	**	***	**	**	ns
vs. Mock					

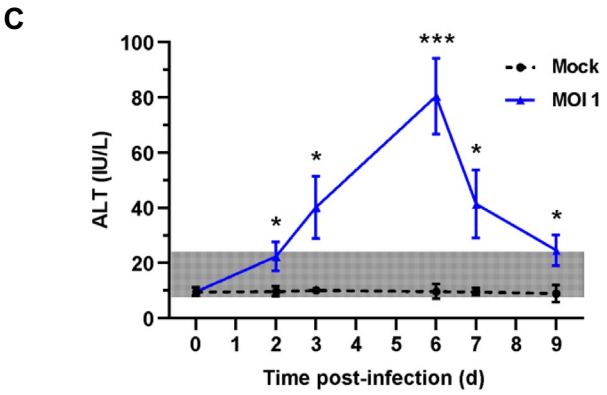

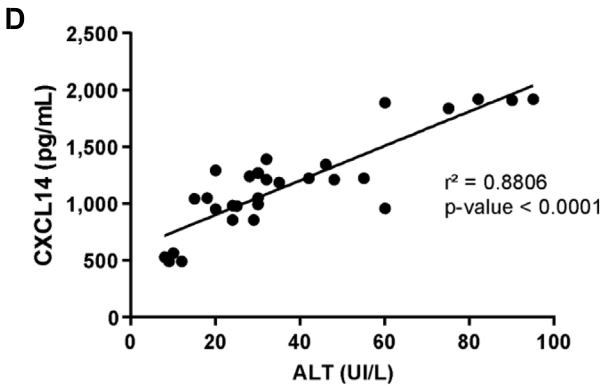

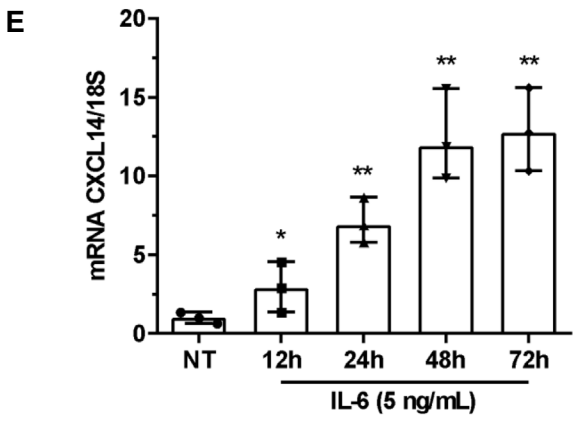

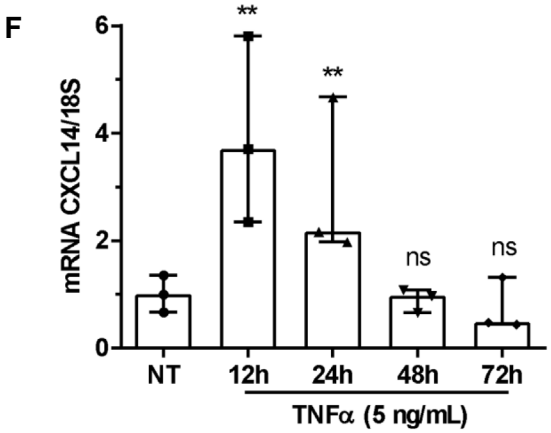

FIGURE 2 | Legend on next page.

FIGURE 2 | Culture of primary murine hepatocytes overexpress CXCL14 when infected with MHV-3 or stimulated with IL-6 and TNFα. PMH were infected with various concentrations of MHV-3 (MOIs of 0.5, 1, or 2) or not (Mock). From day 2 to day 9 after infection, conditioned media and cell lysates were collected. (A) Pictures of PMH cultures, non-infected (Mock) (left) and five days post-infection (5 dpi) with MHV-3 virus at a MOI of 1 (right). (B) Measurement of the CXCL14 concentration in conditioned media of primary murine hepatocytes, non-infected (Mock), or infected with different MOI of MHV-3 (0.5, 1, or 2), after 2, 3, 6, 7 and 9 dpi. Dotted line is the CXCL14 concentration found in mock-infected mice. (C) ALT activity measured in conditioned media of non-infected (Mock) or infected cells at 2, 3, 6, 7, and 9 dpi by MHV-3 at a MOI of 1. Gray area is the normal range of ALT observed in non-treated mice. (D) Correlation between CXCL14 and ALT levels in conditioned media of primary murine hepatocytes infected with MHV-3 at a MOI of 1. (E) Relative expression of CXCL14 mRNA by PMH stimulated with IL-6 or (F) TNFα at 5 ng/mL, after 12, 24, 48 or 72 h post-stimulation. A p-value <0.05 was considered significant: *<0.05, **<0.01, ***<0.001, ns not significant (comparison between mock cells and MHV-3-infected or cytokine-stimulated cells).

significant exponential correlation between CXCL14 and IL-6 with $r^2 = 0.9537$ and $p < 0.0001$ and a linear correlation between CXCL14 and TNFα levels at 72 hpi, with $r^2 = 0.9287$ and $p < 0.0001$ (Figure S3E,F). As observed in Figure S3A–D, mice with low ALT levels (gray dots) highlighted similar values for pro-inflammatory and anti-viral cytokines to the non-infected mice, suggesting a lower level of infection in these mice and rapid control by innate immunity.

Overall, these data suggest that CXCL14 release into the serum is associated with liver damage, in particular with hepatocyte lysis induced by MHV-3 inoculation and with TNFα and IL-6 expression during the inflammatory process of hepatitis.

3.4 | Association Between the CXCL14 Level and the Presence of Immune-Cell Populations in the MHV-3 Mouse Model

We characterized the immune infiltration in the liver during the antiviral response using the MHV-3 model. The total number of immune infiltrating cells in the liver decreased following MHV-3 inoculation (Figure 5A). The proportion and number of $CD4^+$ T cells and NK cells increased significantly after MHV-3 infection (Figure 5B,D), whereas those of NKT cells, macrophages, and neutrophils strongly decreased (Figure 5B,C). There was no significant difference in the number or percentage of $CD8^+$ T cells or B cells following MHV-3 inoculation relative to those of NI mice (Figure 5B,D). Finally, we analyzed immune-cell activation using the marker CD69. More $CD4^+$ T, $CD8^+$ T, B, NK, and NKT cells were activated after MHV-3 inoculation compared with those from NI mice (Figure 5E). Furthermore, there was a strong correlation between CXCL14 serum levels and the percentage of activated cells, with r^2 between 0.8761 and 0.9816 (Figure 5F).

Overall, these results show that infection with MHV-3 induced an active immune response to control viral replication associated with CXCL14 overexpression.

3.5 | No Specific Phenotype for CXCL14-Deficient Mice Highlighted in MHV-3 Induced Acute Hepatitis

CXCL14-deficient mice ($CXCL14^{-/-}$) and their littermate wild-type ($CXCL14^{+/+}$) were infected by MHV-3 at a suboptimal dose to assess a potential function of the chemokine in this model. Following the infection, the body weight of each mouse was measured, and a survival curve was performed (Figure 6A,B). $CXCL14^{-/-}$ and $CXCL14^{+/+}$ lost weight after the infection to reach 90% of their initial body weight at 108 hpi, and mouse survival declines from 72 h post-infection (between 50% and 60% of survival at 108 hpi). However, no significant difference between the two genotypes was observed in body weight loss and the survival curve. Viral production was assessed with an RT-qPCR of the MHV-3 nucleocapsid (Figure 6C). At 72 hpi, the genome equivalent of MHV-3 increased in both genotypes (10^6 GEq) without a significant difference between the two genotypes. Furthermore, to evaluate the effect of CXCL14 on the hepatic damages, ALT measurement was performed (Figure 6D) and HES staining was made in liver sections (Figure 6E, only one representative slide is shown). As shown in Figure 6D, over the time of infection, ALT values increased without a significant difference between $CXCL14^{+/+}$ and $CXCL14^{-/-}$ mice. The histological analysis and the quantification of the necrotic areas (Figure 6F) led to the same conclusion. At 72 hpi, less than 20% of the liver tissue was necrotic, and at 108 hpi, major necrotic areas were observed in $CXCL14^{+/+}$ and $CXCL14^{-/-}$ mice, accounting for 70% of the liver tissue.

In conclusion, by using the MHV-3 acute hepatitis model, no specific function of the CXCL14 chemokine was highlighted. This is most probably because MHV-3 induces a fulminant hepatitis, and all the processes are too fast to observe a moderate phenotype. Furthermore, MHV-3 targets the hepatocytes but also the sinusoidal cells and, unfortunately, the macrophages. Then, it induces a bias in analyzing the immune response in this context. To complete the analysis of CXCL14 chemokine function, we decided to use another strain of MHV, the MHV-A59 virus, that led to a mild disease and whose target cells in the liver are the hepatocytes only.

3.6 | CXCL14 Deficient Mice Are Partially Protected in MHV-A59 Induced Acute Hepatitis

$CXCL14^{-/-}$ mice and their littermate wild-type ($CXCL14^{+/+}$) were infected with hepatic coronavirus MHV-A59. Mice were daily monitored, and the body weight loss was followed (Figure 7A). As shown in this figure, the $CXCL14^{+/+}$ mice showed a decrease in body weight from 1 to 4 dpi and have reached a plateau of approximately 10% body weight loss at 4 dpi. Interestingly, the $CXCL14^{-/-}$ mice lost weight right after the infection (10%) but started to gain weight from 4 dpi to 7 dpi (to initial body weight). We also controlled the welfare to determine

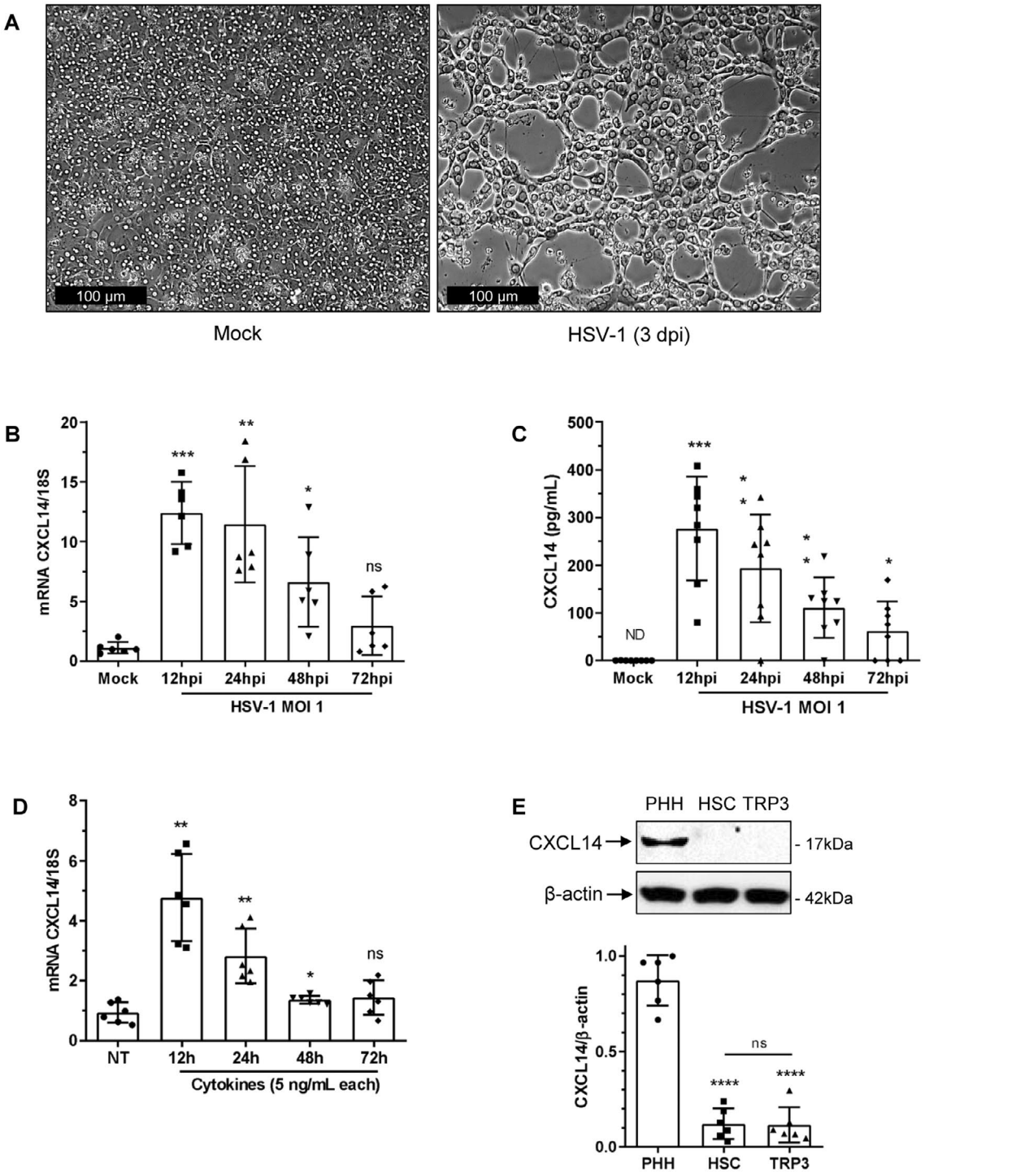

FIGURE 3 | Primary human hepatocytes overexpress and release CXCL14 when infected by HSV-1 or stimulated with pro-inflammatory cytokines. PHH were infected with HSV-1 with a MOI of 1, or not (Mock). From twelve hours to seventy-two hours after, conditioned media and cell lysates were collected. (A) Pictures of PHH, non-infected (Mock) (left) or at 3 dpi with HSV-1 (right). (B) Relative expression of CXCL14 mRNA measured by RT-qPCR in non-infected (Mock) or infected cells at 12, 24, 48, or 72 hpi with HSV-1. (C) Measurement of CXCL14 concentration in conditioned media of PHH cultures of non-infected (Mock) cells or of cells infected with HSV-1 by ELISA at 12, 24, 48, and 72 hpi. (D) Relative expression of CXCL14 mRNA measured by RT-qPCR in non-treated (NT) or PHH cultures stimulated with a cocktail of cytokines (IL-6, TNFα, IL-1β, IFNγ, and OSM at 5 ng/mL each) for 12, 24, 48, or 72 h. (E) Top, western blot of CXCL14 of lysates of non-infected PHH, primary human hepatic stellate cells (HSC), and TRP3, a cell line of human liver sinusoidal endothelial cells (LSEC). Bottom, relative quantification of western-blot signals of CXCL14 production by PHH, HSC, and TRP3. A p-value < 0.05 was considered significant: *< 0.05, **< 0.01, ***< 0.001, ****< 0.0001, ns not significant (comparison between mock cells with HSV-1-infected or cytokine-stimulated cells, or between PHH and HSC or TRP3).

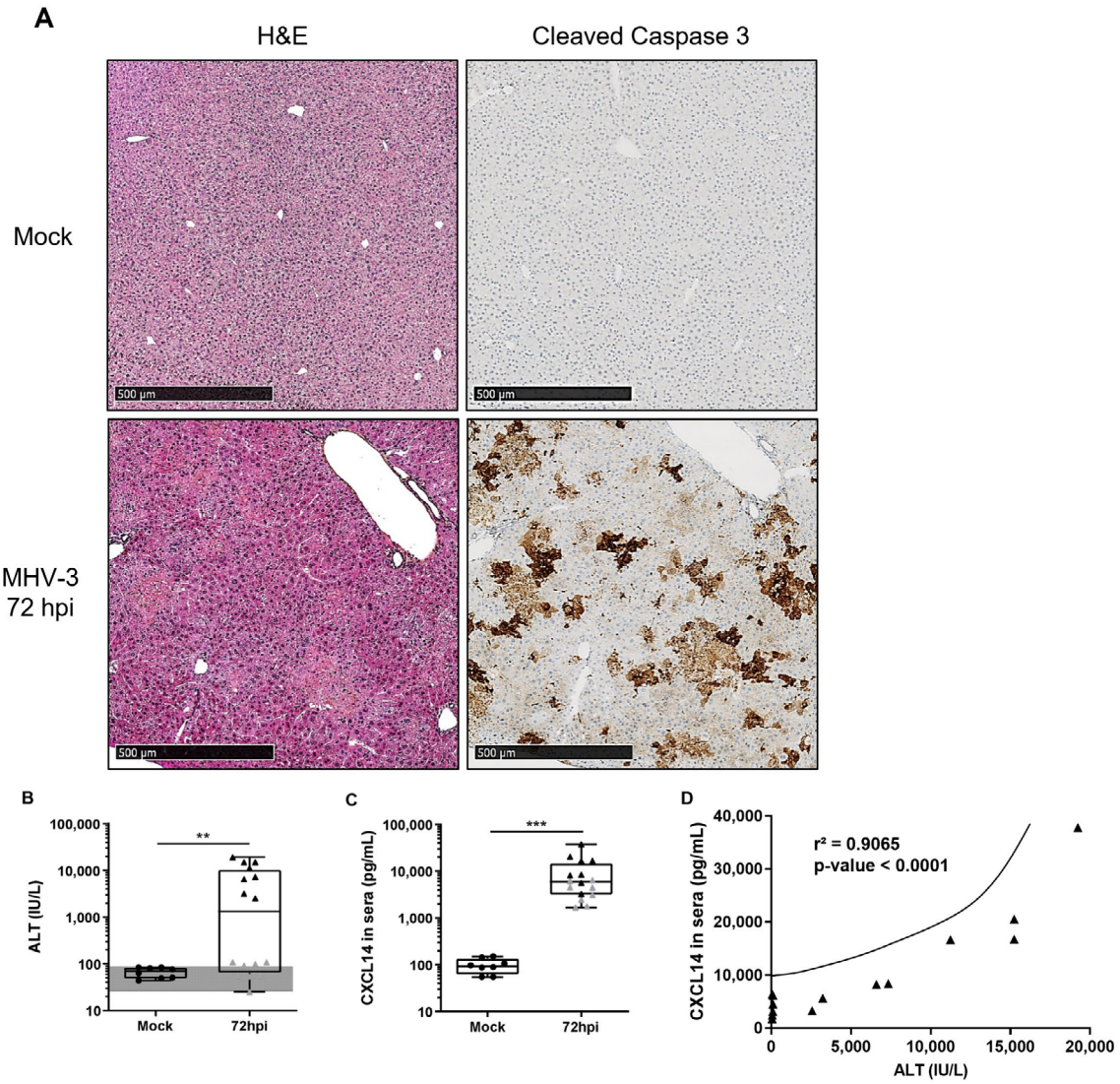

FIGURE 4 | Increase in CXCL14 expression is associated with the intensity of hepatitis in mice in MHV-3-induced fulminant hepatitis model. Mice were injected intraperitoneally either with DPBS (Mock) or with MHV-3. 72 h after, mice were euthanized to collect the liver and the serum. (A) H&E staining (left) and cleaved-caspase 3 immunolabeling (right) in the livers of control (Mock) and MHV-3-infected mice (72 hpi). (B) ALT levels in the sera of control (Mock) and MHV-3-infected mice (72 hpi). Gray area is the normal range of ALT observed in non-treated mice. (C) Titration of CXCL14 in the sera of control (Mock) and MHV-3-infected mice by ELISA (72 hpi). (D) Exponential correlation curve between ALT and CXCL14 levels in the sera of MHV-3-infected mice 72 hpi. A p-value <0.05 was considered significant: **<0.01, ***<0.001 (comparison between Mock mice and MHV-3 infected mice).

a clinical score for each mouse (Figure 7B), and the CXCL14$^{+/+}$ mice highlighted significantly increased scores at 4 dpi and 5 dpi in comparison with the CXCL14$^{-/-}$ mice.

Next, we evaluated the MHV titers in the liver of infected mice at 3 dpi and 7 dpi (Figure 7C). As observed, CXCL14$^{-/-}$ mice featured significantly lower titers at 3 dpi in comparison with the CXCL14$^{+/+}$ mice, respectively, 3000 and 10 000 PFU/sample. At 7 dpi, the same observation is done, with 70 PFU/sample for CXCL14$^{-/-}$ mice and 1000 PFU/sample for the CXCL14$^{+/+}$ mice.

We measured the ALT level in MHV-A59 infected mice to evaluate the liver damage (Figure 7D). CXCL14$^{+/+}$ showed an elevated level of ALT at 3 dpi, close to 2000 UI/L, whereas the CXCL14$^{-/-}$ showed a significantly lower value with an average level at 800 UI/L. At 7 dpi, the ALT levels were at 700 UI/L for the CXCL14$^{+/+}$ mice and about 150 UI/L for the CXCL14$^{-/-}$ mice, which confirmed the tendency at 3 dpi. We also assessed the liver damage by performing an H&E staining from liver sections of mice in the two groups (only one representative slide is shown). As shown in the Figure S4A, at 3 dpi, the liver of CXCL14$^{+/+}$ mice exhibited many cell death areas with immune cell infiltrates (black arrow). In comparison, only a few so-called necrosis areas associated with immune infiltrates were found on liver sections of CXCL14$^{-/-}$ mice. The staining was also performed on liver sections at 7 dpi, and similar observations were made (Figure S4B). The ratio of necrosis area to normal tissue was calculated for each group, as observed in Figure 7E; low ratios of dead tissue were found at 3 dpi for both CXCL14$^{+/+}$ and CXCL14$^{-/-}$ mice. However, at 7 dpi, these ratios were strongly increased for the CXCL14$^{+/+}$ mice and were significantly higher than those for the CXCL14$^{-/-}$ mice.

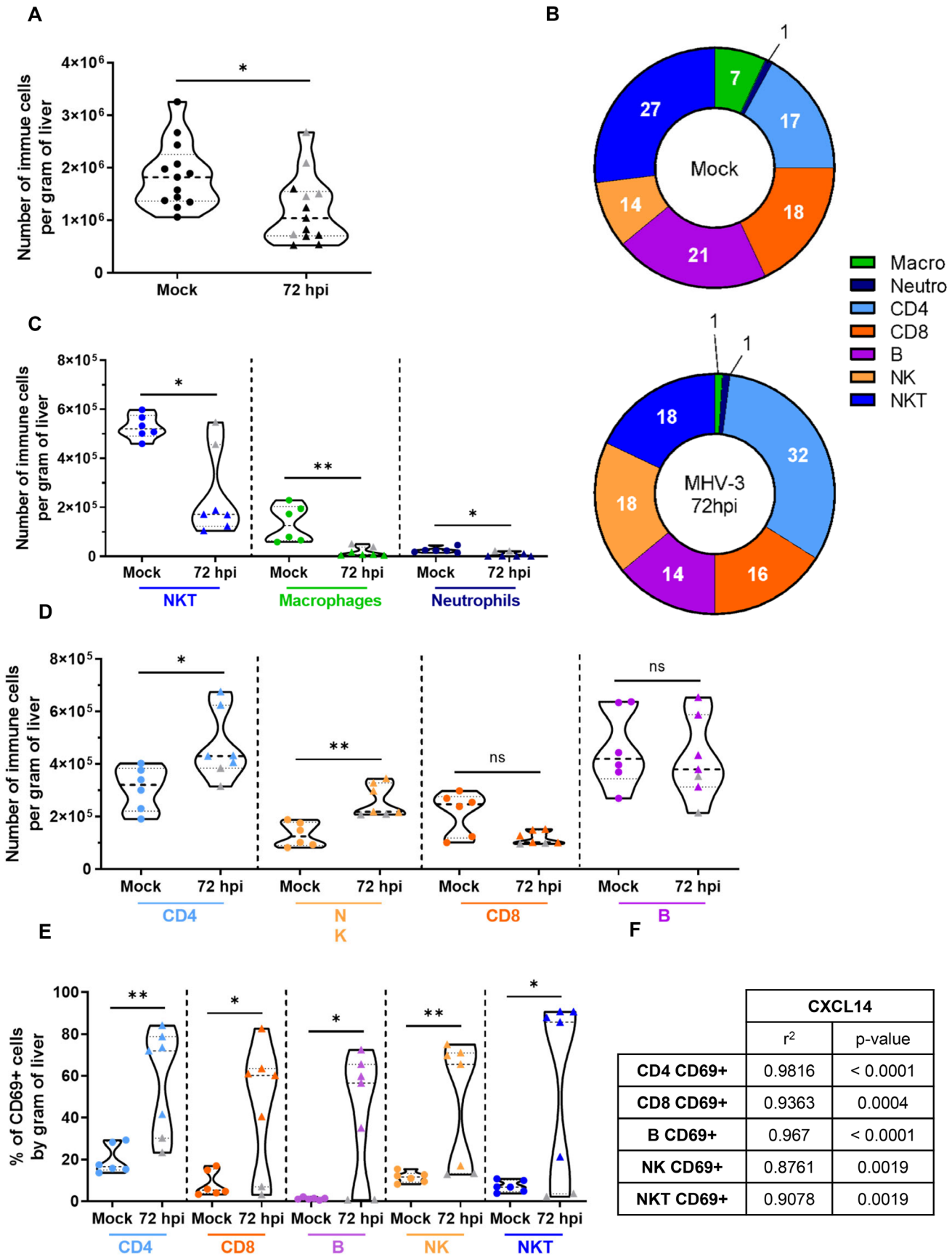

	CXCL14	
	r^2	p-value
CD4 CD69+	0.9816	< 0.0001
CD8 CD69+	0.9363	0.0004
B CD69+	0.967	< 0.0001
NK CD69+	0.8761	0.0019
NKT CD69+	0.9078	0.0019

FIGURE 5 | Legend on next page.

FIGURE 5 | CXCL14 expression is associated with the activation of immune cells in the acute hepatitis MHV-3 model. Mice were injected intraperitoneally either with DPBS (Mock) or with MHV-3. 72 h after, mice were euthanized to harvest the liver and to extract immune cells. (A) Quantification of immune cells by flow-cytometry in the livers of Mock and 72 hpi MHV-3-infected mice. (B) Percentage of each cell population (CD4, CD8, B, NK, and NKT, macrophages, and neutrophils) in the liver of mock and MHV-3-infected mice. (C) Percentage of NKT, macrophages, and neutrophils in the liver of mock and MHV-3-infected mice. (D) Percentage of T CD4+, NK, T CD8+, and B cells in the liver of mock and MHV-3-infected mice. (E) Percentage of CD69 labeled immune cells (CD4, CD8, B, NK, and NKT) in the liver of mock and MHV-3-infected mice. (F) Correlation between CXCL14 serum concentration and percentage of activated cells (T CD4+, T CD8+, B, NK, and NKT). A p-value < 0.05 was considered significant: *< 0.05, **< 0.01, ***< 0.001, ns not significant (comparison between Mock mice and MHV-3 infected mice at 72 hpi).

As demonstrated before, TNFα and IL-6 cytokines are modulatory molecules in the MHV infection model. Here, we measured their concentrations in the sera of MHV-A59 CXCL14$^{+/+}$ and CXCL14$^{-/-}$ infected mice (Figure 7F). CXCL14$^{+/+}$ mice exhibited significantly higher levels of TNFα and IL-6 at 3 dpi and 7 dpi compared to the CXCL14$^{-/-}$ mice, about 2 or 2.5 times higher. The major inflammatory cytokines were measured in the sera of CXCL14$^{+/+}$ and CXCL14$^{-/-}$ mice after MHV-A59 infection (Figure S5B). As observed, cytokine levels were increased at day 3, but not at day 7, with significantly higher values in CXCL14$^{+/+}$ mice for IFNα, CCL2, CCL5, and CXCL10. About IFNγ and IL-10, the CXCL14$^{-/-}$ mice exhibited significantly higher concentrations of these cytokines at 3 and 7 dpi. No difference between genotypes was observed for IL-1β and IL-12p70; however, these cytokines featured higher concentrations at day 3 compared to day 7 post-infection.

Finally, we assessed by flow cytometry the potential function of CXCL14 in the recruitment and activation of hepatic immune cells. As shown in Figure 7G, at 3 dpi, mice exhibit a transient neutrophil recruitment in the liver, with a higher percentage of these cells in the CXCL14$^{-/-}$ mice. Seven days after MHV-A59 infection, CXCL14$^{-/-}$ mice showed a significantly higher amount of CD4^{+} T cells and a significantly lower percentage of macrophages in comparison with the CXCL14$^{+/+}$ mice. No difference was observed for B, CD8^{+} T, NK, and NKT cell percentages in the liver (Figure S5A) as for the CD69 level of expression, an indicator of immune cell activation.

Immunohistochemistry was performed on liver sections from infected mice at 3 and 7 dpi to support the data from the flow-cytometry analysis. As shown in Figure 7H (and Figure S6A), the staining by myeloperoxidase demonstrated that the quantity of neutrophils was strongly increased in the liver of CXCL14$^{-/-}$ mice at 3 dpi and is significantly higher than that of CXCL14$^{+/+}$ mice. This value is decreased at 7 dpi for both genotypes, as observed by flow cytometry. The immunostaining with FoxP3 highlighted an increase in the regulatory T cell population (Treg) following MHV-A59 infection (Figures 7I and S6B), with a higher quantity of Treg in the liver from CXCL14$^{-/-}$ mice at 7 dpi. Finally, the staining with F4/80 (Figures 7J and S6C) shows an increased recruitment of macrophages in the liver of CXCL14$^{+/+}$ mice at 3 dpi and 7 dpi in comparison with CXCL14$^{-/-}$ mice, and this recruitment increased over time after infection.

All together, these data suggest that MHV-A59-infected mice exhibited a worse phenotype in the presence of CXCL14 than in the absence of the chemokine, with increased liver damage and markers of inflammation. Therefore, CXCL14 may be considered a biomarker of poor prognosis in viral hepatitis in mice.

3.7 | CXCL14 Levels Are Associated With the Release of ALT Into the Sera of Patients With Viral Hepatitis

Finally, we evaluated whether CXCL14 release is associated with acute hepatitis in humans. CXCL14 levels were measured in the sera of 61 patients with acute viral hepatitis caused by various viruses or in the sera of 139 patients with acute non-viral hepatitis and 36 healthy donors. Characteristics such as age range, sex, and transaminase activity of the subjects are presented in Table 1. The 61 infected human samples, including those used in Chalin et al. study [29] completed with 39 new patients with viral hepatitis, consisted of 26 HAV, 9 HBV, 22 HEV, and 4 HSV samples. There was no significant difference between the non-viral and viral groups or healthy donors for all clinical parameters, except for ALT and AST levels linked to hepatitis and liver damage.

Serum CXCL14 levels, measured by ELISA, were significantly higher in the sera of patients with viral hepatitis than those in the sera of healthy donors and non-viral hepatitis patients (Figures 8A and S7). The mean CXCL14 serum concentrations were 100 and 150 pg/mL for healthy donors and the non-viral hepatitis group, respectively, and reached 1000 pg/mL in the sera of the viral hepatitis group. CXCL14 levels measured in groups of viral hepatitis patients differentiated by virus type ranged from 1400 pg/mL to nearly 8000 pg/mL (Figure 8B).

We also examined the correlation between CXCL14 concentrations and ALT levels in the acute viral hepatitis group of patients (Figure 8C). There was no correlation between these two parameters for patients infected with HAV, HBV, or HEV. However, there was a positive correlation between CXCL14 and ALT levels in the sera of patients with acute HSV hepatitis, with $r^2 = 0.985$ and $p = 0.007$.

We evaluated by using ROC curves the specificity and the sensitivity of CXCL14 level depending on the etiology of hepatitis, viral group, and non-viral group (Figure 8D). As shown in this figure, CXCL14 showed nonspecific and non-sensitive data for non-viral hepatitis with an AUC equal to 0.5188 and a non-significant p-value equal to 0.7321. However, CXCL14 was significantly sensitive and specific for viral hepatitis with an area under the ROC curve (AUC) equal to 0.9071 and a p-value

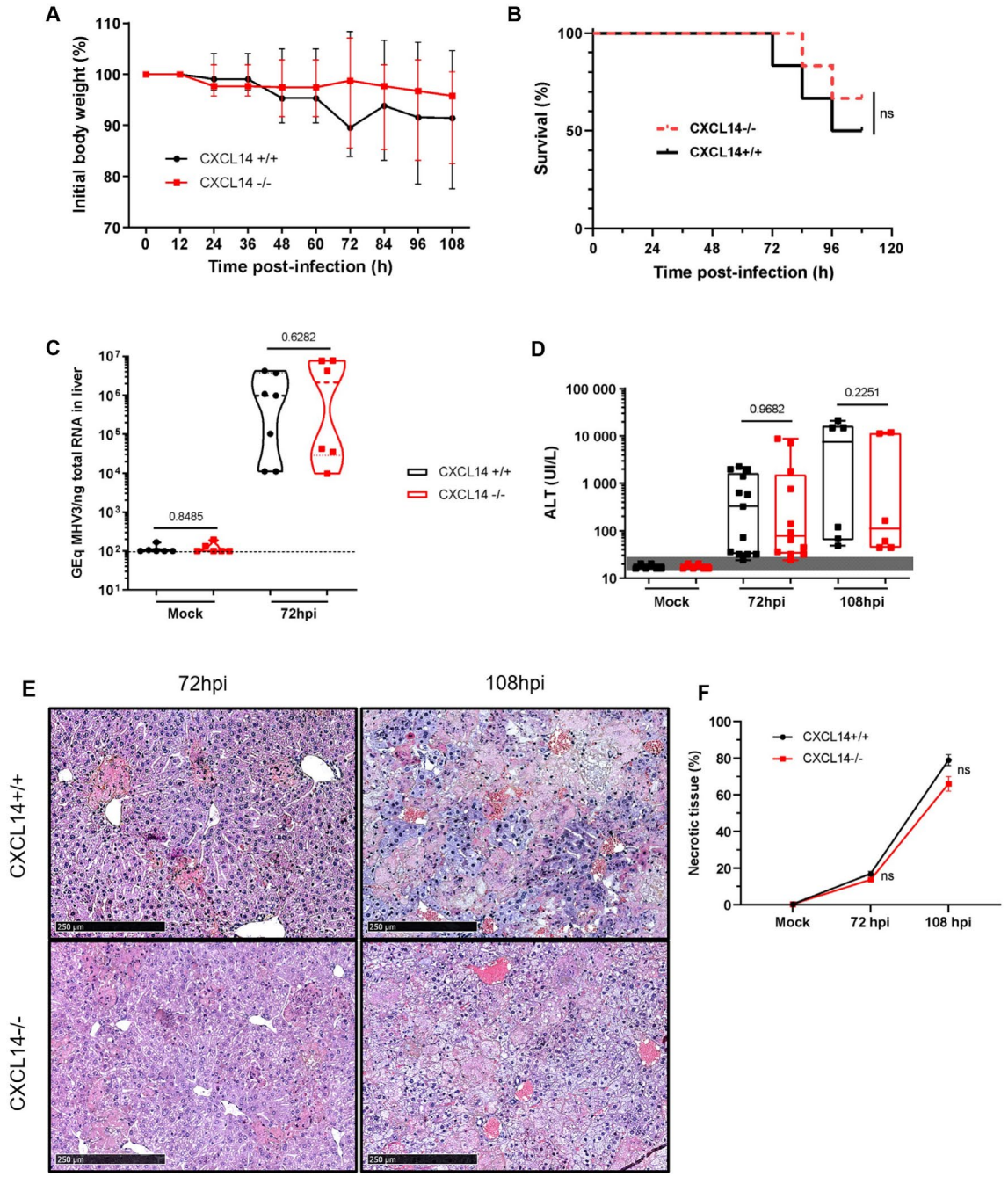

FIGURE 6 | CXCL14$^{+/+}$ and CXCL14$^{-/-}$ mice exacerbate the same phenotype after infection with the MHV-3. CXCL14$^{+/+}$ (blue) and CXCL14$^{-/-}$ (red) mice were injected intraperitoneally either with DPBS (Mock) or with MHV-3. Seventy-two and hundred-eight hours later, mice were euthanized to harvest the liver and the serum. (A) Body weight loss of CXCL14$^{+/+}$ and CXCL14$^{-/-}$ mice after MHV-3 challenge until 108 hpi. (B) Survival curve of CXCL14$^{+/+}$ and CXCL14$^{-/-}$ mice after MHV-3 challenge until 108 hpi. (C) RT-qPCR of MHV-3 nucleocapsid in liver of mock and MHV-3 infected mice at 72 hpi. Dotted line is the limit of detection (100 GEq MHV-3/ng of total RNA in liver). (D) ALT levels in the sera of mock mice and MHV-3-infected mice at 72 hpi and 108 hpi. Gray area is the normal range of ALT observed in non-treated mice. (E) H&E staining from liver sections of CXCL14$^{+/+}$ (top) and CXCL14$^{-/-}$ (bottom) infected mice at 72 hpi and 108 hpi. For all panels, the scale bar is equal to 250 µm. (F) Percentage of necrotic tissue for CXCL14$^{+/+}$ and CXCL14$^{-/-}$ infected or not with MHV-3 in H&E staining. A p-value > 0.05 was considered not significant (ns) (comparison between mock mice and MHV-3 infected mice).

inferior to 0.0001. CXCL14 seems to be particularly relevant for HSV fulminant hepatitis.

In conclusion, these patient data show that the increase in CXCL14 serum levels is associated with severe hepatic injury induced by viral liver infection in humans and suggest a specific inflammatory mechanism during viral hepatitis that is distinct from the one involved in non-viral hepatitis. Importantly, these data suggest that CXCL14 can discriminate between hepatitis of viral and non-viral etiology in humans.

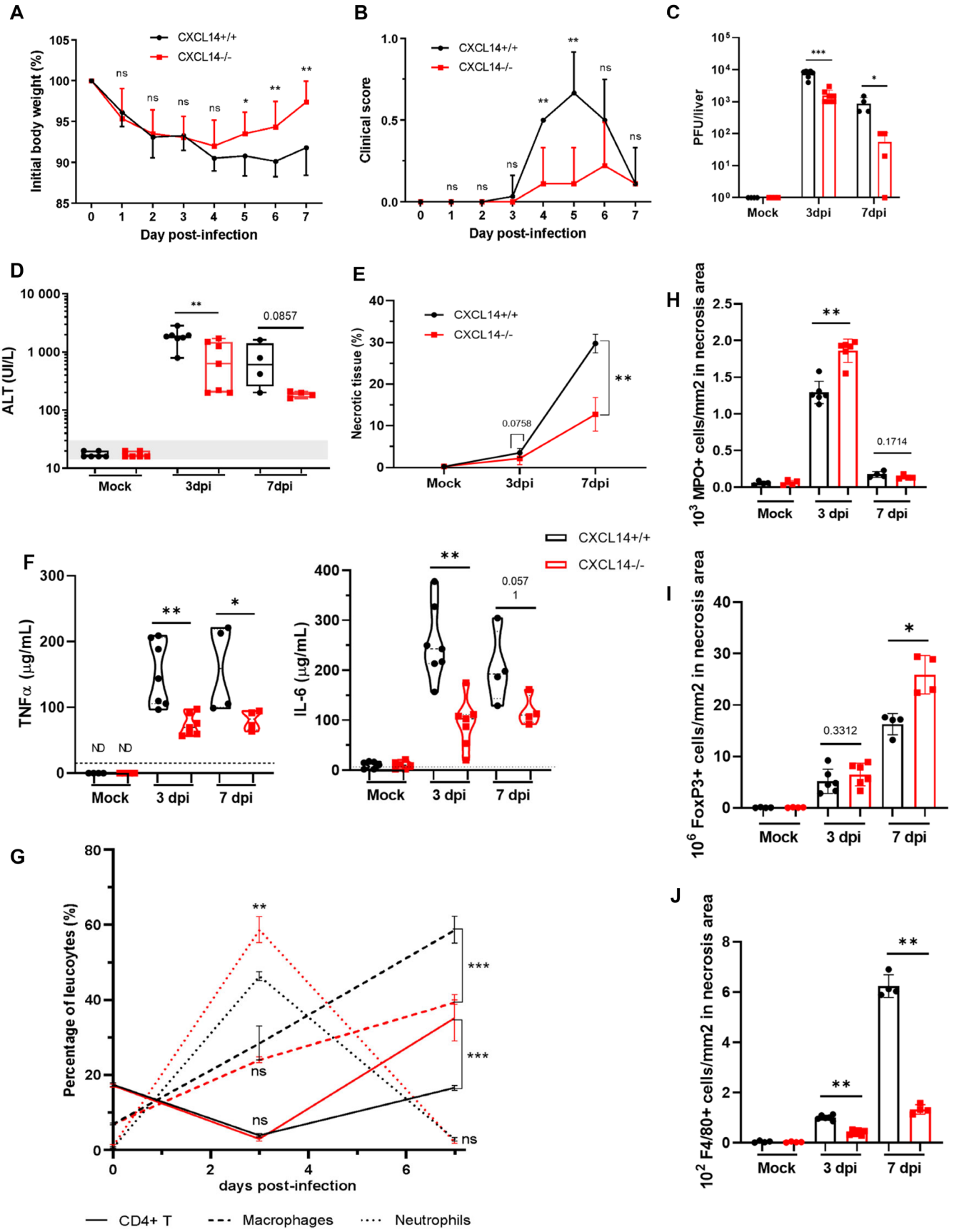

FIGURE 7 | Legend on next page.

FIGURE 7 | CXCL14$^{-/-}$ mice are partially protected against MHV-A59 infection. CXCL14$^{+/+}$ (blue) and CXCL14$^{-/-}$ (red) mice were infected with MHV-A59 at 5000 PFU intraperitoneally. At 3 dpi and 7 dpi, mice were euthanized and samples were collected. (A) Body weight loss of CXCL14$^{+/+}$ and CXCL14$^{-/-}$ mice after MHV-A59 challenge until 7 dpi. (B) Observed animal clinical score of CXCL14$^{+/+}$ and CXCL14$^{-/-}$ mice after MHV-A59 challenge until 7 dpi. (C) MHV-A59 viral titration by plaque assay from liver of Mock mice and infected mice at 3 dpi and 7dpi. (D) ALT levels in the sera of MHV-A59 infected mice (3 and 7 dpi) and mock-infected mice. Gray area is the normal range of ALT observed in non-treated mice. (E) Ratio of necrotic tissue to the normal tissue calculated on liver sections at 0, 3, and 7dpi. (F) Measurement of IL-6 and TNFα cytokines in the sera of mock-infected mice or MHV-A59-infected mice 3 dpi and 7dpi. (G) Relative quantification of immune cells (percentage of leucocytes) by flow-cytometry in the liver of MHV-A59-infected mice before infection and at 3 dpi and 7dpi. Percentage of CD4 cells (CD3$^+$, CD8$^-$, and CD4$^+$), macrophages (CD19$^-$, CD3$^-$, NK1.1$^-$, Gr1$^-$, and CD11b$^+$) and neutrophils (CD19$^-$, CD3$^-$, NK1.1$^-$, Gr1$^+$, and CD11b$^+$). (H–J) Quantification of myeloperoxidase (MPO), FoxP3, or F4/80 positive cells per mm^2 in necrosis area of liver sections, respectively. A p-value <0.05 was considered significant: *<0.05, **<0.01, ***<0.001, ns not significant (comparison between CXCL14$^{+/+}$ and CXCL14$^{-/-}$ mice infected by MHV-A59).

TABLE 1 | Main characteristics of the cohort: number of cases, sex ratio, mean age, and ALT and AST levels.

	Healthy donors	Non viral patients	Viral patients
Case (*n*)	36	139	61
Sex (M/F)	21/15	101/38	45/16
Age (year) average (min–max)	48 (33–65)	53 (13–99)	47 (15–82)
ALT (IU/L) average (min–max)	22.2 (12–42)	1205 (134–8587)	2452 (140–9874)
AST (IU/L) average (min–max)	25.3 (16–40)	1215 (32–11 369)	2018 (86–7628)

4 | Discussion

Human mortality associated with infection with hepatotropic viruses, such as HAV, HBV, HCV, HDV, and HEV, is increasing worldwide. Immunity plays a key role in resolving such viral infections. Among the actors of immunity, we focused on the chemokine CXCL14. Indeed, we found CXCL14 to be overexpressed in the livers of mice infected with a virus responsible for fulminant hepatitis. We aimed to understand the regulation and expression of CXCL14 during viral hepatitis and the role of CXCL14 in inflammation following viral infection.

We demonstrate that, in the liver, CXCL14 is expressed by hepatocytes but not by endothelial cells or hepatic stellate cells, suggesting that hepatocytes in the liver are the major source of CXCL14, as already observed by the human atlas consortium (www.proteinatlas.org). CXCL14 is ubiquitously and abundantly expressed in various normal epithelial tissues, such as those in the digestive and urinary tracts, placenta, tongue, breast, kidney, and skin [13, 18]. The expression of CXCL14 is generally down-regulated in inflammatory processes, indicating that it plays an important role in the maintenance of tissue homeostasis [30]. However, we found that IL-6 and TNFα are able to induce CXCL14 transcript and protein levels in PMH. During hepatitis, characterized by an active inflammation process, IL-6 and TNFα are known to be overexpressed. Indeed, CXCL14 levels were also elevated and were closely correlated to those of IL-6 and TNFα in MHV infected mice, suggesting a regulation loop between these cytokines in the context of viral hepatitis. In other in vitro models, it has been shown that CXCL14 expression can be inhibited by inflammatory stimuli, such as TNFα in epithelial tissues [13]. The molecular mechanisms governing CXCL14 expression are still unclear, and the discovery of its receptor and target cells will help in the understanding of the expression and role of this chemokine. Then, we showed that CXCL14 serum concentration was significantly increased in humans or mice infected with hepatotropic viruses, compared with non-infectious liver diseases. This observation suggested a specific role of CXCL14 in the inflammatory response in the context of liver viral infection.

Surprisingly, we have been unable to measure CXCL14 protein in conditioned media without cell lysis, even when the CXCL14 transcript was upregulated following pro-inflammatory cytokine stimulation. Cytokines and chemokines are usually released during classical degranulation from secretory granules previously packaged for storage in the Golgi, although the secretion of IL-1 family cytokines after inflammasome activation appears to be related to membrane permeability disruption [31]. The mode of CXCL14 secretion is still unknown. Here, we demonstrate, in vitro in mice and humans, that CXCL14 is released after cell lysis induced by viral infection with MHV-3 or HSV-1, and we hypothesize that this cell lysis is responsible for the massive release of CXCL14 into the bloodstream in vivo. This way of secretion allows us to classify CXCL14 as an alarmin, like IL-33, HMGB1, S100 protein, or IL-1β [32, 33]. In fact, these cytokines are released following infection and act as immune system activators, leading to tissue repair (cytokines production and immune cell recruitment) but also to the development of acute or chronic inflammatory responses with uncontrolled inflammation.

In patients, CXCL14 is overexpressed in the acute inflammatory context of hepatitis, which differs from chronic viral hepatitis, for which we have not observed overexpression (unpublished data). Moreover, the best correlation between

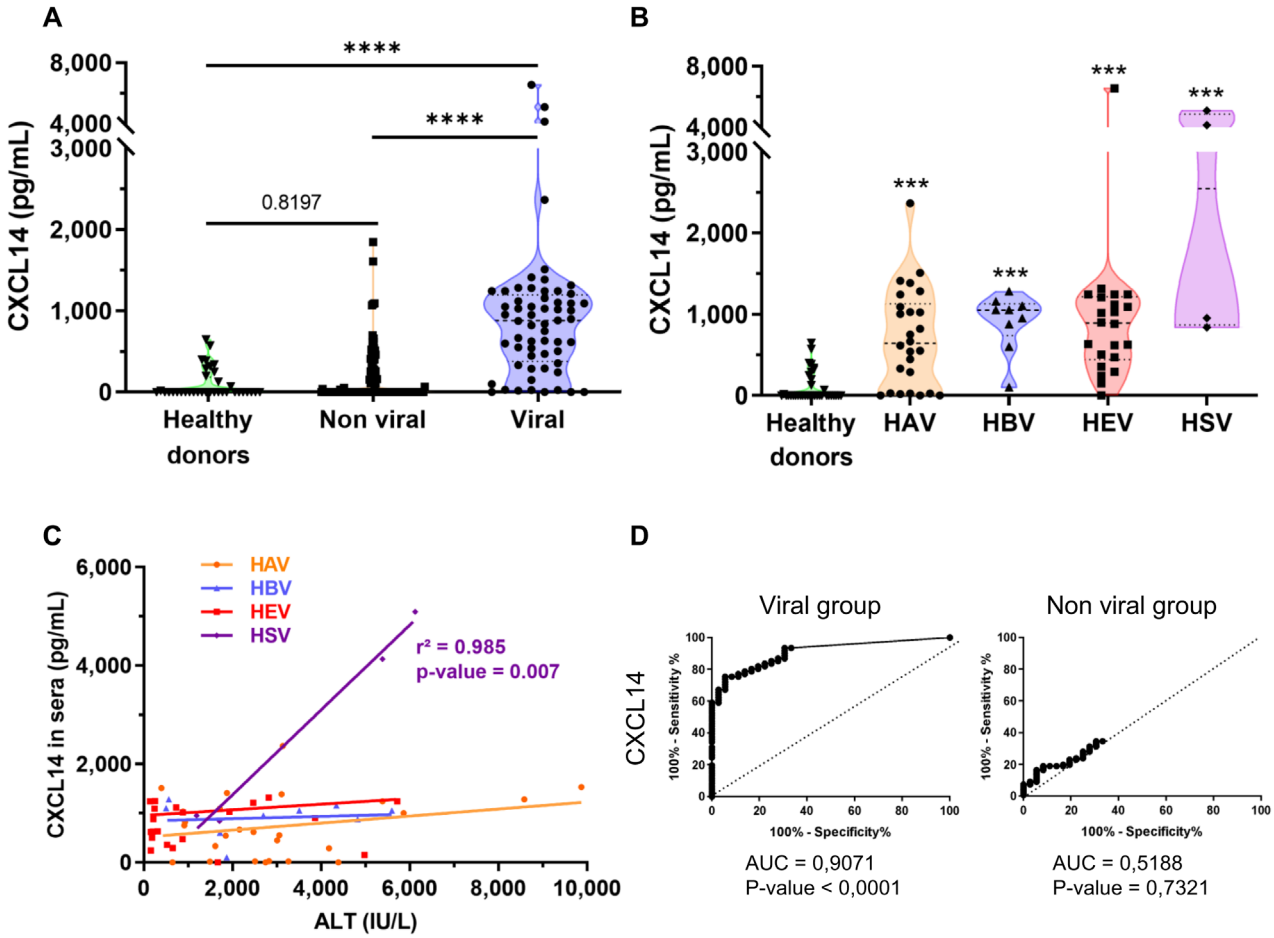

FIGURE 8 | Elevated CXCL14 levels in the sera of patients with acute viral hepatitis. Serum of patients with acute hepatitis and healthy donors were collected to measure CXCL14 concentration and transaminase levels. (A) Quantification of CXCL14 in the sera of healthy donors, patients with non-viral hepatitis, and patients with viral hepatitis. (B) Quantification of CXCL14 in the sera of healthy donors and patients with viral hepatitis, depending on the virus causing the hepatitis. (C) Correlation between CXCL14 concentration and ALT activity in the sera of patients with acute viral hepatitis, according to the virus. (D) ROC curve of CXCL14 in the group of patients with viral hepatitis (left) or non-viral hepatitis (right). AUC and *p*-value are shown on the graph. A *p*-value <0.05 was considered significant: ***<0.001, ****<0.0001 (comparison between healthy donors and acute hepatitis patients).

transaminase levels, the gold standard of hepatocyte lysis, and those of serum CXCL14 was obtained in HSV-infected patients probably because HSV is the most lytic virus of hepatocytes in humans. Altogether, the data suggest that the CXCL14 level seems to be directly linked with the ALT level and cell lysis degree in patients. The ROC curves showed that CXCL14 could be used as a biomarker of acute viral hepatitis in patients, which complements the information provided by measuring ALT only. However, this is not specific for viral infection as Umbaugh et al. also measured significantly high levels of CXCL14 in the sera of patients undergoing acute liver failure following acetaminophen (APAP) overdose [34]. The control group of 139 non-viral hepatitis patients in our study (Figure S7) includes only 7 cases of APAP intoxication, which show moderate ALT and CXCL14 serum levels below 400 pg/mL. These cannot be directly compared to the cases in Umbaugh's study, where patients displayed severe liver injury and CXCL14 serum levels exceeding 2000 pg/mL. By using 2 cohorts of survivors and non-survivors, Umbaugh et al. were able to demonstrate the predictive value of high circulating CXCL14 levels for poor prognosis of APAP-induced acute liver failure. Taking Umbaugh et al. 's data together with our own, CXCL14 levels appear to be indicative of significant inflammation and liver degeneration, which supports our hypothesis that the release of this chemokine in large quantities results from hepatocyte damage.

Finally, we looked for an association between CXCL14 expression and immune cells present in the liver during viral hepatitis using the MHV-3 infected mouse model. Here, we found that the expression of CXCL14 is strongly associated with the number of activated T lymphocytes (CD4 and CD8), activated B lymphocytes, and activated NK and NKT cells. Moreover, CXCL14 expression is also linked with antiviral cytokines such as IFNs and TNF. However, the MHV-3 infection led to a fulminant hepatitis in 3 days with a massive destruction of hepatocytes but also macrophages [19]. To assess the function of CXCL14 in vivo, we used the MHV-A59 infection model in mice knock-out or not for CXCL14. With this model, we show that CXCL14$^{+/+}$ mice were sicker than the CXCL14$^{-/-}$, with higher ALT values and an exacerbated inflammatory response with high concentrations in sera for IL-6 and TNF. In contrast, in the absence of CXCL14,

the level of IL-10 was increased and the recruitment of neutrophils, macrophages, and T regulatory cells was significatively modified. These data suggest a regulation loop of the inflammatory response in those mice, involving regulatory T lymphocytes as the population of macrophages is reduced. CXCL14 was described as a biomarker of hepatocellular carcinoma and positively correlated with immune cell infiltration and chemokines abundance [35]. In another model of inflammation, it has been demonstrated that CXCL14 is an immunomodulator involved in the stroke-induced inflammatory response by regulating immature dendritic cells and regulatory T cells accumulation [36]. Taken together, these published data and our data suggest that CXCL14 could have a role in preventing T regulatory cells mobilization supporting inflammation burst.

However, Umbaugh et al. [34, 37] recently demonstrated that CXCL14 is also produced in both humans and mice following an APAP overdose. Their studies suggest that CXCL14 is produced by $p21^+$ peri-necrotic hepatocytes, which may contribute to hepatocyte injury and hinder regeneration. The two hepatitis models are quite distinct. The APAP model relies on direct hepatocyte toxicity, which is eventually amplified by inflammatory cells such as neutrophils and macrophages. In contrast, MHV-induced hepatitis depends on cytotoxic lymphocytes to induce hepatocyte death through an adaptive immune response. Immunohistochemistry of MHV-infected mice livers did not reveal any $p21^+$ hepatocytes, unlike in APAP-treated mice livers. Therefore, CXCL14 plays a different role in the APAP toxicity model, where it may recruit macrophages to eliminate senescent hepatocytes, than in MHV-induced hepatitis, where CXCL14 may play a role in preventing the recruitment of regulatory T cells, thereby supporting the inflammatory response.

In conclusion, our studies demonstrate that CXCL14 is regulated by IL-6 and TNFα is released into the blood by hepatocyte lysis and is associated with a strong lymphocyte antiviral immune response and the release of pro-inflammatory and antiviral cytokines. CXCL14 could therefore be considered a novel indicator of inflammation and liver injury in mice and humans infected with acute viral hepatitis.

Author Contributions

Christelle Devisme, Claire Piquet-Pellorce, Arnaud Chalin, and Michel Samson conceived and designed the study. Claire Piquet-Pellorce, Charaf Benarafa, and Michel Samson supervised the project. Michel Samson obtained funding. Benjamin Lefevre, Charlotte Pronier, and Vincent Thibault provided human biological material. Charaf Benarafa provided murine strain. Christelle Devisme, Claire Piquet-Pellorce, Arnaud Chalin, Jacques Le Seyec, and Céline Raguénès-Nicol performed all the experiments. Christelle Devisme, Arnaud Chalin, Charlotte Pronier, Vincent Thibault, and Céline Raguénès-Nicol analyzed the data. Christelle Devisme, Claire Piquet-Pellorce, Céline Raguénès-Nicol, and Michel Samson drafted figures and the manuscript, with critical review and approval by all authors.

Acknowledgments

We would like to thank Lucie Fonteneau for her technical assistance. We acknowledge the "Laboratoire de Biochimie-Toxicologie" from the "CHU de Rennes" for transaminase measurements. For histological analysis, bead-based immunoassays, and animal house facilities, we would like to thank the dedicated platforms (i.e., H2P2, flow-cytometry and cell sorting, and ARCHE) of SFR Biosit—UMS 3480, US_S 018, France.

Conflicts of Interest

The authors declare no conflicts of interest.

Data Availability Statement

The data that support the findings of this study are available in the materials and methods, results, and/or Supporting Information of this article.

References

1. K. R. Mysore and D. H. Leung, "Hepatitis B and C," *Clinics in Liver Disease* 22 (2018): 703–722.

2. F. Cui, S. Blach, C. Manzengo Mingiedi, et al., "Global Reporting of Progress Towards Elimination of Hepatitis B and Hepatitis C," *Lancet Gastroenterology & Hepatology* 8 (2023): 332–342.

3. S. Belkaya, E. Michailidis, C. B. Korol, et al., "Inherited IL-18BP Deficiency in Human Fulminant Viral Hepatitis," *Journal of Experimental Medicine* 216 (2019): 1777–1790.

4. F. Marra and F. Tacke, "Roles for Chemokines in Liver Disease," *Gastroenterology* 147 (2014): 577–594.e1.

5. C. Benarafa and M. Wolf, "CXCL14: The Swiss Army Knife Chemokine," *Oncotarget* 6 (2015): 34065–34066.

6. J. Mikulak, E. Bruni, F. Oriolo, C. Di Vito, and D. Mavilio, "Hepatic Natural Killer Cells: Organ-Specific Sentinels of Liver Immune Homeostasis and Physiopathology," *Frontiers in Immunology* 10 (2019): 946.

7. M. Afify, A. H. Hamza, and R. A. Alomari, "Correlation Between Serum Cytokines, Interferons, and Liver Functions in Hepatitis C Virus Patients," *International Society for Interferon and Cytokine Research* 37, no. 1 (2017): 32–38, https://doi.org/10.1089/jir.2016.0044.

8. C. E. Samuel, "Antiviral Actions of Interferons," *Clinical Microbiology Reviews* 14 (2001): 778–809.

9. A. Apolinario, P. L. Majano, E. Alvarez-Pérez, et al., "Increased Expression of T Cell Chemokines and Their Receptors in Chronic Hepatitis C: Relationship With the Histological Activity of Liver Disease," *American Journal of Gastroenterology* 97 (2002): 2861–2870.

10. X. Cao, W. Zhang, T. Wan, et al., "Molecular Cloning and Characterization of a Novel CXC Chemokine Macrophage Inflammatory Protein-2 Gamma Chemoattractant for Human Neutrophils and Dendritic Cells," *Journal of Immunology* 165, no. 5 (2000): 2588–2595, https://doi.org/10.4049/jimmunol.165.5.2588.

11. M. O. Huising, T. van der Meulen, G. Flik, and B. M. L. Verburg-van Kemenade, "Three Novel Carp CXC Chemokines Are Expressed Early in Ontogeny and at Nonimmune Sites," *European Journal of Biochemistry* 271 (2004): 4094–4106.

12. G. Al Hamwi, V. Namasivayam, B. Büschbell, R. Gedschold, S. Golz, and C. E. Müller, "Proinflammatory Chemokine CXCL14 Activates MAS-Related G Protein-Coupled Receptor MRGPRX2 and Its Putative Mouse Ortholog MRGPRB2," *Communications Biology* 7 (2024): 52.

13. S. Meuter and B. Moser, "Constitutive Expression of CXCL14 in Healthy Human and Murine Epithelial Tissues," *Cytokine* 44 (2008): 248–255.

14. M. A. Sleeman, J. K. Fraser, J. G. Murison, et al., "B Cell- and Monocyte-Activating Chemokine (BMAC), a Novel Non-ELR Alpha-Chemokine," *International Immunology* 12 (2000): 677–689.

15. C. Dai, P. Basilico, T. P. Cremona, et al., "CXCL14 Displays Antimicrobial Activity Against Respiratory Tract Bacteria and Contributes to

Clearance of *Streptococcus pneumoniae* Pulmonary Infection," *Journal of Immunology* 194, no. 12 (2015): 5980–5989, https://doi.org/10.4049/jimmunol.1402634.

16. T. Hara and K. Tanegashima, "Pleiotropic Functions of the CXC-Type Chemokine CXCL14 in Mammals," *Journal of Biochemistry (Tokyo)* 151, no. 5 (2012): 469–476, https://doi.org/10.1093/jb/mvs030.

17. T. Starnes, K. K. Rasila, M. J. Robertson, et al., "The Chemokine CXCL14 (BRAK) Stimulates Activated NK Cell Migration: Implications for the Downregulation of CXCL14 in Malignancy," *Experimental Hematology* 34 (2006): 1101–1105.

18. C. Maerki, S. Meuter, M. Liebi, et al., "Potent and Broad-Spectrum Antimicrobial Activity of CXCL14 Suggests an Immediate Role in Skin Infections," *Journal of Immunology (Baltimore, Md.: 1950)* 182, no. 1 (2009): 507–514, https://doi.org/10.4049/jimmunol.182.1.507.

19. L. Lamontagne, J. P. Descoteaux, and P. Jolicoeur, "Mouse Hepatitis Virus 3 Replication in T and B Lymphocytes Correlate With Viral Pathogenicity," *Journal of Immunology* 142, no. 12 (1989): 4458–4465, https://doi.org/10.4049/jimmunol.142.12.4458.

20. A. Jacques, C. Bleau, C. Turbide, N. Beauchemin, and L. Lamontagne, "A Synergistic Interferon-Gamma Production Is Induced by Mouse Hepatitis Virus in Interleukin-12 (IL-12)/IL-18-Activated Natural Killer Cells and Modulated by Carcinoembryonic Antigen-Related Cell Adhesion Molecules (CEACAM) 1a Receptor," *Immunology* 128 (2009): e551–e561.

21. C. Bleau, A. Filliol, M. Samson, and L. Lamontagne, "Mouse Hepatitis Virus Infection Induces a Toll-Like Receptor 2-Dependent Activation of Inflammatory Functions in Liver Sinusoidal Endothelial Cells During Acute Hepatitis," *Journal of Virology* 90 (2016): 9096–9113.

22. M. I. Arshad, S. Patrat-Delon, C. Piquet-Pellorce, et al., "Pathogenic Mouse Hepatitis Virus or Poly(I:C) Induce IL-33 in Hepatocytes in Murine Models of Hepatitis," *PLoS One* 8, no. 9 (2013): e74278, https://doi.org/10.1371/journal.pone.0074278.

23. C. Devisme, M. Stosskopf, C. Piquet-Pellorce, et al., "Interleukin-18 Binding Protein (IL-18BP) Deficiency Affects Lymphocyte Activation and IL-18 Expression in a Mouse Model of Liver Inflammation," *European Journal of Immunology* 55 (2025): e202451579.

24. R. W. Körner, M. Majjouti, M. A. A. Alcazar, and E. Mahabir, "Of Mice and Men: The Coronavirus MHV and Mouse Models as a Translational Approach to Understand SARS-CoV-2," *Viruses* 12, no. 8 (2020): 880, https://doi.org/10.3390/v12080880.

25. Z. Yang, J. Du, G. Chen, et al., "Coronavirus MHV-A59 Infects the Lung and Causes Severe Pneumonia in C57BL/6 Mice," *Virologica Sinica* 29 (2014): 393–402.

26. M. Farooq, A. Filliol, M. Simoes Eugénio, et al., "Depletion of RIPK1 in Hepatocytes Exacerbates Liver Damage in Fulminant Viral Hepatitis," *Cell Death & Disease* 10 (2019): 1–12.

27. M. Régeard, M. Trotard, C. Lepère, P. Gripon, and J. Le Seyec, "Entry of Pseudotyped Hepatitis C Virus Into Primary Human Hepatocytes Depends on the Scavenger Class B Type I Receptor," *Journal of Viral Hepatitis* 15 (2008): 865–870.

28. V. Carrière, M. I. Arshad, J. Le Seyec, et al., "Endogenous IL-33 Deficiency Exacerbates Liver Injury and Increases Hepatic Influx of Neutrophils in Acute Murine Viral Hepatitis," *Mediators of Inflammation* 2017 (2017): 1359064.

29. A. Chalin, B. Lefevre, C. Devisme, et al., "Serum CXCL10, CXCL11, CXCL12, and CXCL14 Chemokine Patterns in Patients With Acute Liver Injury," *Cytokine* 111 (2018): 500–504.

30. I. Kurth, K. Willimann, P. Schaerli, T. Hunziker, I. Clark-Lewis, and B. Moser, "Monocyte Selectivity and Tissue Localization Suggests a Role for Breast and Kidney-Expressed Chemokine (BRAK) in Macrophage Development," *Journal of Experimental Medicine* 194, no. 6 (2001): 855–861, https://doi.org/10.1084/jem.194.6.855.

31. V. S. Tapia, M. J. D. Daniels, P. Palazón-Riquelme, et al., "The Three Cytokines IL-1β, IL-18, and IL-1α Share Related but Distinct Secretory Routes," *Journal of Biological Chemistry* 294 (2019): 8325–8335.

32. D. Bertheloot and E. Latz, "HMGB1, IL-1α, IL-33 and S100 Proteins: Dual-Function Alarmins," *Cellular & Molecular Immunology* 14 (2017): 43–64.

33. M. I. Arshad, C. Piquet-Pellorce, and M. Samson, "IL-33 and HMGB1 Alarmins: Sensors of Cellular Death and Their Involvement in Liver Pathology," *Liver International* 32, no. 8 (2012): 1200–1210, https://doi.org/10.1111/j.1478-3231.2012.02802.x.

34. D. S. Umbaugh, N. T. Nguyen, S. C. Curry, et al., "The Chemokine CXCL14 Is a Novel Early Prognostic Biomarker for Poor Outcome in Acetaminophen-Induced Acute Liver Failure," *Hepatology* 79, no. 6 (2024): 1352–1364, https://doi.org/10.1097/HEP.0000000000000665.

35. Y. Lin, B.-M. Chen, X.-L. Yu, H.-C. Yi, J.-J. Niu, and S.-L. Li, "Suppressed Expression of CXCL14 in Hepatocellular Carcinoma Tissues and Its Reduction in the Advanced Stage of Chronic HBV Infection," *Cancer Management and Research* 11 (2019): 10435–10443, https://doi.org/10.2147/CMAR.S220528.

36. H.-T. Lee, S.-P. Liu, C.-H. Lin, et al., "A Crucial Role of CXCL14 for Promoting Regulatory T Cells Activation in Stroke," *Theranostics* 7 (2017): 855–875.

37. D. S. Umbaugh, N. T. Nguyen, S. H. Smith, A. Ramachandran, and H. Jaeschke, "The p21+ Perinecrotic Hepatocytes Produce the Chemokine CXCL14 After a Severe Acetaminophen Overdose Promoting Hepatocyte Injury and Delaying Regeneration," *Toxicology* 504 (2024): 153804.

Supporting Information

Additional supporting information can be found online in the Supporting Information section.